Numerical study on the resonance response of spar-type floating platform in 2-D surface wave

Eung-Young Choi[1], Jin-Rae Cho[*2] and Weui-Bong Jeong[3]

[1]*KFX Airframe Analysis Team, Korea Aerospace Industries, Sacheon 52529, Republic of Korea*
[2]*Department of Naval Architecture and Ocean Engineering, Hongik University,
Sejong 339-701, Republic of Korea*
[3]*School of Mechanical Engineering, Pusan National University, Busan 609-735, Republic of Korea*

Abstract. This paper is concerned with the numerical study on the resonance response of a rigid spar-type floating platform in coupled heave and pitch motion. Spar-type floating platforms, widely used for supporting the offshore structures, offer an economic advantage but those exhibit the dynamically high sensitivity to external excitations due to their shape at the same time. Hence, the investigation of their dynamic responses, particularly at resonance, is prerequisite for the design of spar-type floating platforms which secure the dynamic stability. Spar-type floating platform in 2-D surface wave is assumed to be a rigid body having 2-DOFs, and its coupled dynamic equations are analytically derived using the geometric and kinematic relations. The motion-variance of the metacentric height and the moment of inertia of floating platform are taken into consideration, and the hydrodynamic interaction between the wave and platform motions is reflected into the hydrodynamic force and moment and the frequency-dependent added masses. The coupled nonlinear equations governing the heave and pitch motions are solved by the RK4 method, and the frequency responses are obtained by the digital Fourier transform. Through the numerical experiments to the wave frequency, the resonance responses and the coupling in resonance between heave and pitch motions are investigated in time and frequency domains.

Keywords: spar-type floating platform; 2-D surface wave; heave and pitch motions; coupled nonlinear equations; coupling in resonance

1. Introduction

Floating platforms are widely used to support various offshore structures at sea, such as floating offshore wind turbines and storage/offloading platforms, using their buoyancy. Several types of floating platforms have been introduced so far, but, among them, spar-type is commonly preferred thanks to its excellent vertical posture stability and the relatively simple shape and the easy installation at deep sea (Roddier *et al*. 2010, Chujo *et al*. 2011). However, it suffers from the inherent dynamic instability induced by wave and wind loads at the same time because it is not fixed on ground but floating at sea (Irani and Finn 2004, Jeon *et al*. 2013, Browning *et al*. 2014). Here, the dynamic instability is mostly meant by the pitch and roll motions and the heave motion in the vertical direction. The dynamic instability including the unstable station-keeping of floating platform owing to wave and wind loads may not only deteriorate the target performance but also lead to the fatal structural failure of entire offshore structure. In this regard, the securing of dynamic stability is essential for the successful application of spar-type floating platform to the

offshore engineering (Tong 1998, Faltinsen 1990).

As a sort of fluid-structure interaction problem involving an exterior liquid sloshing, the dynamic motion of spar-type floating platform accompanies the complicate interaction between buoyancy, translation and rotational inertia forces and hydrodynamic pressure. In aspect of geometry, spar-type floating platform is characterized by the small waterplane area compared to the submerged volume, so that it is not easily excited vertically and displays heave and pitch motions of relatively long natural periods (Rho 2002). However, at resonance, the heave motion dramatically increases and induces the large coupled pitch motion, which gives rise to a disadvantageous effect on the restoring moment (Karimirad *et al*. 2011, Ryo *et al*. 2002a). The change of restoring moment causes the time delay and results in the phase change in the heave motion, and the stability of spar-type floating platform in such environments was assessed based on the Mathieu-type instability (Ryo *et al*. 2002b, Haslum and Faltinsen 1999). To design a spar-type floating platform which secures the dynamic stability, the investigation of its dynamic responses, particularly at resonance, becomes the first and most important step. It has been reported that the coupling between heave and pitch/roll motions causes the coupling in resonance (Matos *et al*. 2011) as well as the primary resonances at the heave and pitch natural frequencies.

According to our literature survey restricted to floating

∗Corresponding author, Professor
 E-mail: jrcho@hongik.ac.kr

platform, Liao and Yeung (2001) investigated the nonlinear effects, associated with bilge keels and fluid viscosity, on the roll response of cylinder in wave by a time-domain viscous-fluid method. They found that the response characteristics are very different depending on whether or not bilge keels and fluid viscosity are considered. Rho *et al.* (2002b) performed the free-decay tests in a wave tank with a scaled model to determine the natural periods and damping coefficients, and the motions in regular waves. They observed that pitch motions become unstable when the pitch natural period is double the heave natural period. Koo *et al.* (2004) evaluated damping effects and hull/mooring/riser effects on the principle instability. They considered the heave/pitch coupling using the modified Mathieu equation and investigated the wave elevation effect on Mathieu instability. Hong *et al.* (2005) performed experiments on the extreme motions of a spar platform in heave resonant waves in a water basin. They observed that unstable roll and pitch motions are occurred when the periods of wave are close to the heave resonant period and twice of the roll/pitch natural periods. Kyoung *et al.* (2005) created a test model for floating platforms and performed numerous tests in scenarios involving regular waves of various frequencies. They provided experimental verification of the occurrence of coupling in resonance with unstable pitch motion, when the frequency of vibrations becomes close to twofold the natural frequency of pitch. Radhakrishnan *et al.* (2007) measured the motion of a tethered spherical buoy subjected to incident regular wave in a wave tank, and they observed the transverse instability when the period of the wave generated was close to one-half of the natural period of the buoy. Matos *et al.* (2011) computed the second-order resonant heave, roll and pitch motions by means of a commercial BEM code and compared with those measured in small-scale tests performed in a wave basin. Ye *et al.* (2014) investigated the hydrodynamic performances of two FOWT scale modes, one cylindrical spar and the other with heave plate at the bottom. They present the numerical and test results for the regular and irregular waves, and they found the difference of the cylindrical spar with heave plate exists between numerical and test owing to the behavior of the heave plate.

Most of previous studies concerned with the instability and coupled resonance were performed by scale model experiment in water basin or by numerical analysis using complex software. In order words, the previous work relied on the cost- and time-consuming experiment or the complicated time-consuming (within dozens of hours) numerical computation, in order to evaluate the dynamic responses of floating platform. In this context, the purpose of current study is to present a time-effective numerical method to analyze the parametric resonance of 2-D spar-type floating platform in coupled heave and pitch motion. The time- and frequency-responses of spar platform can be rapidly (within dozens of minutes) obtained by solving a nonlinear dynamic equations expressed by only two degrees of freedom. Thus, the present numerical method could be usefully employed for the modeling of spar floating platform that is free from the coupled resonance. As an

extension of our previous work on the spar-type floating platform (Jeon *et al.* 2013, Choi *et al.* 2015), the resonance response of a rigid spar-type floating platform in 2-D surface wave is solved by the coupled nonlinear equations which are derived using the geometric and kinematic relations of floating platform. And, the hydrodynamic force and moment acting on the floating platform are derived in terms of the velocity potential for 2-D incompressible and inviscid surface wave, in which the motion dependence of the metacentric height and the moment of inertia of floating platform are considered. The hydrodynamic interaction between the rigid floating platform and 2-D wave is modeled as the frequency and motion dependent added masses (Cho *et al.* 2001). The transient dynamic responses of the spar-type floating platform in heave and pitch motions are numerically solved using the fourth-order Runge-Kutta (RK-4) method and transformed into the frequency domain by the digital Fourier transform. The numerical experiments are performed with respect to the wave frequency in order to investigate the resonance responses and the coupling in resonance between heave and pitch motions.

2. Spar-type floating platform in 2-D surface wave

Let us consider 2-D incompressible, irrotational and inviscid surface wave of the wave length λ, the wave amplitude η_a and the mean water depth h. The unsteady flow velocity $\boldsymbol{v} = \{u, w\}$ of water particles is governed by the Bernoulli equation (Currie 1974) expressed by

$$\frac{1}{2}(u^2 + w^2) + \frac{p}{\rho} + gz + \frac{\partial \phi}{\partial t} = 0 \qquad (1)$$

with the hydrodynamic pressure $p(x, z; t)$ and the velocity potential $\phi(x, z)$. The flow velocity satisfies the non-penetration condition at bottom surface, which is given by

$$w = \frac{\partial \phi}{\partial z} = 0 \ \ at \ z = -h \qquad (2)$$

and the kinematic and dynamic boundary conditions given by

$$w = \frac{\partial \eta}{\partial t} + u \frac{\partial \eta}{\partial x} \ \ at \ \ z = \eta_a \qquad (3)$$

$$\frac{1}{2}(u^2 + w^2) + g\eta + \frac{\partial \phi}{\partial t} = 0 \ \ at \ z = \eta_a \qquad (4)$$

at the mean surface $(z = 0)$ with ρ and g being the water density and the gravitational acceleration. The wave height $\eta = \eta(x; t)$ in 2-D surface wave is defined by $\eta(x; t) = \eta_a cos(\kappa x - \omega t)$ with κ being the wave number and ω being the angular frequency.

By assuming 2-D surface wave be small-amplitude, one can derive the wave velocity potential given by

$$\phi = \eta_a \cdot \frac{g}{\omega} \cdot \frac{cosh[\kappa(h+z)]}{cosh(\kappa h)} sin(\kappa x - \omega t) \qquad (5)$$

from the governing Eqs. (1)-(4) (Sorensen 1978, Dean and Dalrymple 1984). Then, from the definition of wave velocity potential, one can derive the directional particle velocities given by

$$u = \frac{\partial \phi}{\partial x} = \eta_a \cdot \frac{\kappa g}{\omega} \cdot \frac{cos[\kappa(h+z)]}{cosh(\kappa h)} \cdot cos(\kappa x - \omega t) \quad (6)$$

$$w = \frac{\partial \phi}{\partial z} = \eta_a \cdot \frac{\kappa g}{\omega} \cdot \frac{sinh[\kappa(h+z)]}{cosh(\kappa h)} \cdot sin(\kappa x - \omega t) \quad (7)$$

Substituting the velocity potential ϕ into the modified kinematic boundary condtion: $\frac{\partial^2 \phi}{\partial t^2} + g \frac{\partial z}{\partial t} = 0$ at the mean surface $(z = 0)$, one can get the dispersion relationship which is expressed in terms of the angular frequency ω and the wave number κ: $\omega^2 = \kappa g \cdot tanh(\kappa h)$.

In case of deep water $(h \to \infty)$, the term $tanh(\kappa h)$ approaches unity and the hyperbolic function terms in Eqs. (5)-(7) become $exp(\kappa z)$, which leads to the following directional water particle velocities given by

$$u = \eta_a \omega \cdot e^{\kappa z} \cdot cos(\kappa x - \omega t) \quad (8)$$

$$w = \eta_a \omega \cdot e^{\kappa z} \cdot sin(\kappa x - \omega t) \quad (9)$$

And, according to the linearized Bernoulli equation, one can derive the wave pressure field $p(x, z; t)$ given by

$$p(x, z, t) = \frac{1}{2} \rho \eta^2 \omega^2 \cdot e^{2\kappa z} + \rho g \eta \cdot e^{\kappa z} \cdot cos(\kappa x - \omega t) (10)$$

Where, the hydrostatic pressure term $\rho g z$ is excluded because it is considered as the initial condition for the hydrodynamic analysis.

Referring to Fig. 1 representing a 2-D cylindrical floating platform in heave and pitch motions, the point O is the origin of Cartesian co-ordinates while other three points *B, G* and *MC* denote the center of buoyancy, the center of gravity and the metacenter. And, D_{eq} and is Δz are the draft (i.e., the length of wet part) and the vertical displacement of gravity center. The platform is assumed to be a rigid undamped body with two degrees-of-freedom. Letting $F = \{F_H, F_V\}$ and M be the hydrodynamic force and moment resultants, the heave motion $z(t)$ and pitch motion $\theta(t)$ around the metacenter MC are governed by

$$m\ddot{z}(t) + k \cdot z(t) = F_V \quad (11)$$

$$I\ddot{\theta}(t) + k_\theta \cdot \theta(t) = M \quad (12)$$
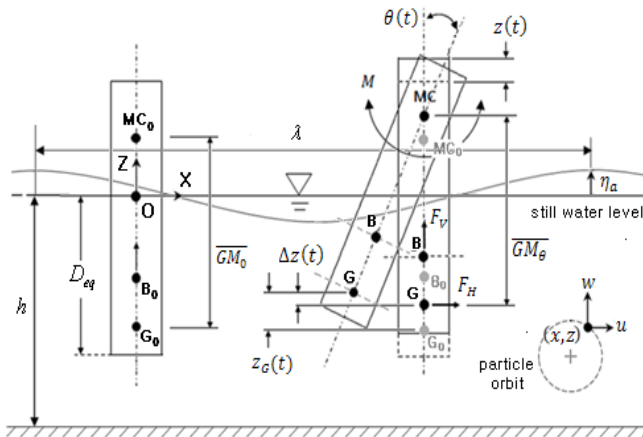
with *m* and *I* being the total mass and the area moment of

inertia. Here, the moment of inertia I of floating platform is defined with respect to the metacenter so that it varies with the motion of floating platform. Meanwhile, the hydrostatic stiffnesses k and k_θ in the heave and pitch motions are defined by $k = \rho g A_w$ and $k_\theta = \rho g \nabla \cdot \overline{GM_\theta}$ with the waterplane area A_w and the metacentric height $\overline{GM_\theta}$. Here, the displacement volume ∇ (i.e., the volume of submerged part) is calculated by $\nabla = A_w \times (D_{eq} - z)$. Note that k_θ is not constant but variable because both ∇ and $\overline{GM_\theta}$ are varying with the motion of floating platform.

From the geometric configuration of the floating platform, the heave displacement $z(t)$ at the metacenter *MC* and the heave displacement $z_G(t)$ at the center of gravity are in the following relationship given by

$$z(t) = z_G(t) - \Delta z(t) = z_G(t) - 2 \cdot \overline{GM_\theta} \cdot sin^2\left(\frac{\theta(t)}{2}\right) (13)$$

The volume change of submerged part according to the platform motion results in the position change of the center of buoyancy, which in turn changes the metacenter. Hence, the metacentric height $\overline{GM_\theta}$ at the pitch angle θ is determined the following relation given by

$$\overline{GM_\theta} = \overline{GMC_0} + \overline{MC_0 MC} = \overline{GM_0} + \frac{1}{2} \cdot \frac{I_w}{\nabla} \cdot tan^2\theta \quad (14)$$

with I_w being the area moment of inertia of the wet part of platform. Here, $\overline{GMC_0}$ and $\overline{MC_0 MC}$ indicate the vertical distances between G and MC_0 and between MC_0 and MC, respectively.

Substituting Eq. (14) into Eq. (13), together with the approximation of $sin^2\theta = tan^2\theta \approx \theta^2$ for small rotation, ends up with

$$z(t) = z_G(t) - \left(\overline{GM_0} + \frac{1}{2} \cdot \frac{I_w}{\nabla} \cdot \theta^2\right) \cdot \frac{\theta^2}{2}$$
$$= z_G(t) - \overline{GM_0} \cdot \frac{\theta^2}{2} \quad (15)$$

$$\ddot{z}(t) = \ddot{z}_G(t) - \overline{GM_0} \cdot (\dot{\theta}^2 + \theta\ddot{\theta}) \approx \ddot{z}_G(t) \quad (16)$$

By substituting these approximate equations into the equation of translation motion (11), one can derive the following approximate equation of heave motion given by

$$m\ddot{z}_G(t) + k\left(z_G(t) - \overline{GM_0} \cdot \frac{\theta^2}{2}\right) = F_V \quad (17)$$

at the center of gravity. Furthermore, by substituting $k_\theta = \rho g \nabla \cdot \overline{GM_\theta}$ into Eq. (12), using the relations in Eqs. (13)-(14), one can derive the approximate equation of pitch motion, which is given by

$$I\ddot{\theta}(t) + k \cdot D_{eq} \cdot \overline{GM_0} \cdot \theta(t) + \frac{1}{2}\left(k \cdot \overline{GM_0}^2 + \rho g I_w\right)$$
$$\cdot \theta^3 - k \cdot \overline{GM_0} \cdot z_G(t) \cdot \theta(t) = M \quad (18)$$

3. Hydrodynamic force and moment

Fig. 2 shows the free body diagram of floating platform, where the radius and the cross-section are denoted by R

Fig. 1 A spar-type floating platform in 2-D progressive surface wave
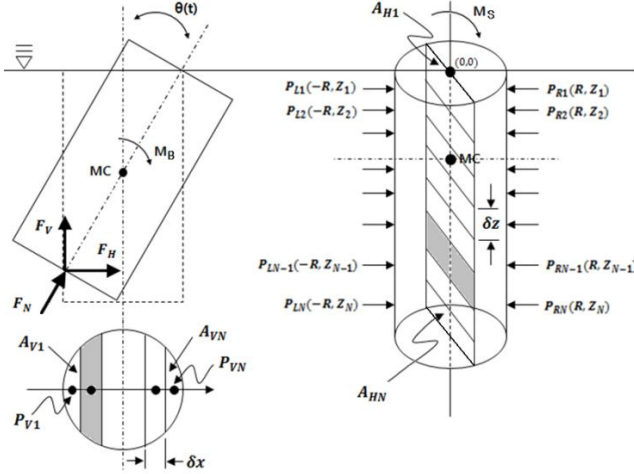
Fig. 2 Free body diagram of the floating platform subject to the hydrodynamic pressure

and A_V, respectively. The surface of floating platform is composed of the bottom surface B and the cylindrical surface S, and the normal force resultant F_N is acting on B while the hydrodynamic pressure acting on S is projected on the left and right sides of the vertical cross-section normal to the wave direction. To calculate the vertical force resultant F_V and moment resultants M_B and M_S, the bottom surface and the cylincrical surface are equally divided into the total of N sub-sections. Each cross-section is assumed to be subject to a force amounting to the central pressure multiplied by its area. For the division $i = 1 \sim N$, the sub-sectional areas A_{Vi} and A_{Hi} on the bottom surface and the projected vertical cross-section are calculated by $A_{Vi} = 2 \cdot \sqrt{R^2 - x^2} \cdot dx$ $A_{Hi} = 2 \cdot R \cdot \delta z$, respectively.

Meanwhile, the co-ordinates (x_i, z_i) of the sampling points within each sub-section are determined by the geometry transformation between the static equilibrium state and the current moving state. Letting (X_i, Z_i) be the sampling points at the static equilibrium and $(0, b)$ be the co-ordinates of metacenter MC at the current moving state, the following geometry transformation

$$x_i = X_i \cdot \cos \theta(t) - (Z_i - b) \cdot \sin \theta(t) \qquad (19)$$

$$z_i = X_i \cdot \sin \theta(t) + (Z_i - b) \cdot \cos \theta(t) + z(t) \qquad (20)$$

according to the translational heave motion $z(t)$ and the rotational pitch motion $\theta(t)$.

The hydrodynamic pressure at a specific position (x', z') on the surface of floating platform under heave and pitch motions is calculated by

$$p(x', z'; t) = \frac{1}{2} \rho \eta^2 \omega^2 \cdot e^{2\kappa z'} + \rho g \eta \cdot e^{\kappa z'} \cdot \cos(\kappa x' - \omega t) \quad (21)$$

Referring to Fig. 2, the normal force F_{Ni} acting on the i-th cross-section AV_i of platform bottom surface B is calculated by

$$F_{Ni} = p(P_{Vi}; t) \cdot A_{Vi} \qquad (22)$$

Then, the vertical force component F_{Vi} and the horizontal force component F_H are expressed by

$$F_{Vi} = F_{Ni} \cdot \cos \theta(t) \qquad (23)$$

$$F_{Hi} = F_{Ni} \cdot \sin \theta(t) \qquad (24)$$

Thus, the moment M_B due to the hydrodynamic pressure acting on the bottom surface B becomes the sum of all the contributions of N cross-sections as follows

$$M_B = \sum_{i=1}^{N} [F_{Vi} \cdot (P_{Vxi} - MC_x) + F_{Hi} \cdot (P_{Vzi} - MC_z)] \quad (25)$$

with (P_{Vxi}, P_{Vzi}) and (MC_x, MC_z) being the positions of P_{Vi} and the metacenter MC.

Meanwhile, on the i-th cross section AH_i of the cylindrical surface S of floating platform, the left and right force components F_{Li} and F_{Ri} are calculated by

$$F_{Li} = p(P_{Li}; t) \cdot A_{Hi} \cdot \cos \theta(t) \qquad (26)$$

$$F_{Ri} = p(P_{Ri}; t) \cdot A_{Hi} \cdot \cos \theta(t) \qquad (27)$$

Then, the moment M_S arising from the difference in the hydrodynamic pressures on the left and right sides can be calculated according to

$$M_S = \sum_{i=1}^{N} F_{Ri} \cdot (P_{Rzi} - MC_z) - \sum_{i=1}^{N} F_{Li} \cdot (P_{Lzi} - MC_z) \quad (28)$$

with P_{Rzi}, P_{Lzi}, MC_z being the z components of P_{Ri}, P_{Li} and MC respectively.

Finally the vibratory force F_V causing the heave motion and the total moment M acting on the floating platform become

$$F_V = \sum_{i=1}^{N} F_{Vi}, \quad M = M_B + M_S \qquad (29)$$

Then, finally Eqs. (17) and (18) can be integrated into the following matrix form of coupled equations for $z_G(t)$ and $\theta(t)$

$$\begin{bmatrix} \tilde{m} & 0 \\ 0 & \tilde{I} \end{bmatrix} \begin{Bmatrix} \ddot{z}_G \\ \ddot{\theta} \end{Bmatrix} + \begin{bmatrix} k & -\frac{1}{2} \cdot \overline{GM_0} \cdot \theta \\ -k \cdot \overline{GM_0} \cdot \theta & \tilde{k} \end{bmatrix} \begin{Bmatrix} z_G \\ \theta \end{Bmatrix} = \begin{Bmatrix} F_V \\ M \end{Bmatrix} \quad (30)$$

with $\tilde{m} = m + m_a$, $\tilde{I} = I + I_a$ and $\tilde{k} = k \cdot D_{eq} \cdot \overline{GM_0} + \frac{1}{2} \left(k \cdot \overline{GM_0}^2 + \rho g I_w \right) \cdot \theta^2$ Here, m_a and I_a indicate the added mass in heave motion and the added moment of inertia in pitch motion. The transient response of Eq. (30) is solved using the fourth-order Runge-Kutta (RK4) method which is numerically implemented by MATLAB.

4. Numerical experiment

In this section, the analytical and numerical formulae derived in Sections 2 and 3 are illustrated through the numerical experiments of a cylindrical floating body. In addition, the resonance characteristics of the body are investigated with respect to the wave excitation frequency.

4.1 Preliminary results

A 1/50-scale cylindrical semi-submersible platform shown in Fig. 3(a) is taken for the numerical experiments, where the diameter D and the total length L of the body are by 20 and 100 m, respectively. The other parameters are as follows: the water density ρ of 1,025 kg/m^3, the
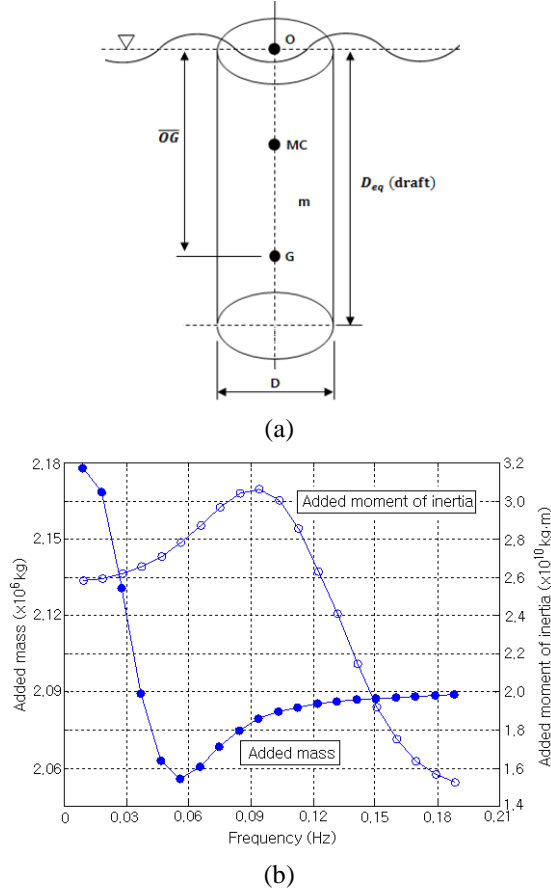
(a)

(b)

Fig. 3 (a) A 1/50 scale platform model, (b) frequency-dependent added mass and added moment of inertia

(a)

(b)

Fig. 4 Transient responses ($\Omega = 0.1 Hz$): (a) heave motion, (b) pitch motion

total mass of structure m of 3.1974×10^7 kg, the draft D_{eq} of 99.34 m, and the COG location $\overline{OG}$ of 60 m, respectively. Here, the draft D_{eq} was determined using the relation of $D_{eq} = m/\rho A_w$. The distributed mass of structure is concentrated to the center of gravity G as a lumped mass, and the above-mentioned parameters were chosen for the simulation model to have the heave and pitch natural frequencies near 0.048 Hz and 0.058 Hz respectively.

Fig. 3(b) represents the variation of added mass and added moment of inertia to the angular velocity that was obtained by AQWA (2012). As is given in Eq. (18), the added mass is reflected to the heave motion while the added moment of inertia to the pitch motion. The variation of total added mass is relatively smaller than the total added mass of inertia, and both show the contrary trend to the angular velocity. One can infer, from the variation of both added quantities, that the heave and pitch motions exhibit the contrary behaviors to the wave excitation. It can be realized to some extent from Figs. 4(a) and 4(b) that represent the transient response of heave and pitch motions when 1-D sinusoidal wave having the frequency of 0.1 Hz and the wave height of 1.0 m is applied. The heave motion displays the repeating events with almost the same peak amplitude and beating pattern, but the pitch motion shows typical cyclic events with the amplitudes ranging from 1.2° to 2.8° without apparent beating.
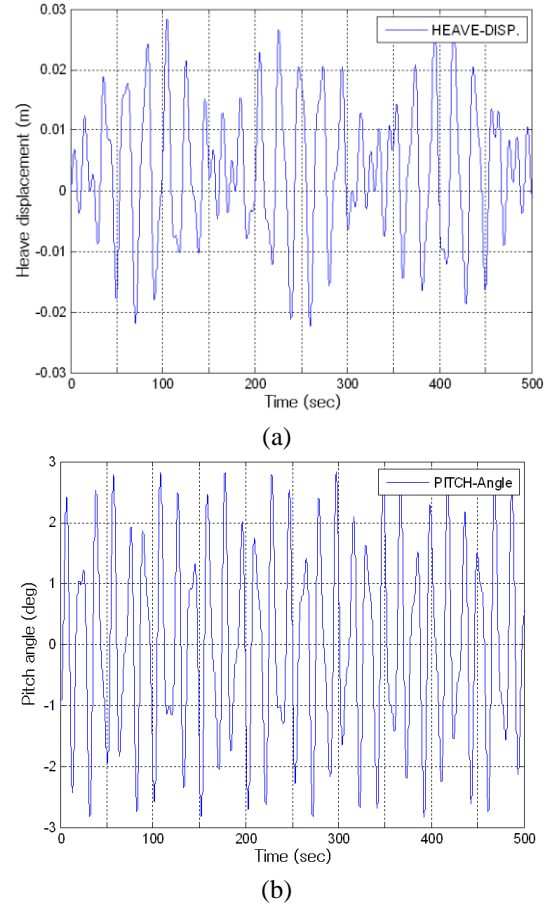
Fig. 5(a) represents the time history of metacentric height $\overline{GM_\theta}$ according to the heave and pitch motions of floating body. It is influenced by the total volume ∇ and moment of inertia I_w of submerged part and the pitch angle θ, as is expressed in Eq. (14), so that its time history is affected by those of heave and pitch motions. However, in our case, it is observed that the time history is more similar to one of pitch motion shown in Fig. 5(b), and the maximum variation is found to be $3.0 x 10^{-4}$ m. Meanwhile, Fig. 5(b) represents the time variation of the area moment of inertia I_w of the wet part, which is observed to be dominated by the time variation of heave motion. It is natural because the amount of wet part is directly proportional to the draft D_{eq} in heave motion, and the maximum variation of I_w is found to be $1.3 x 10^{-4}$ kg · m².

Two plots in Fig. 6 represent the time histories of vertical force resultant F_V and the moment resultant M that are exerted on the floating platform. It is observed that two resultants display the typical sinusoidal (cosine) time variation with the amplitudes of 5.75×10^4 N and 5.75×10^8 N · m, respectively. The peak pitch angle of floating platform is less than 3° as represented in Fig. 4(b) so that all $sin\theta(t)$ and $cos\theta(t)$ terms in Eqs. (23)-(24) and (26)-(27) approach zero or unity. Thus, the time variation of both resultants is dominated by the sinusoidal
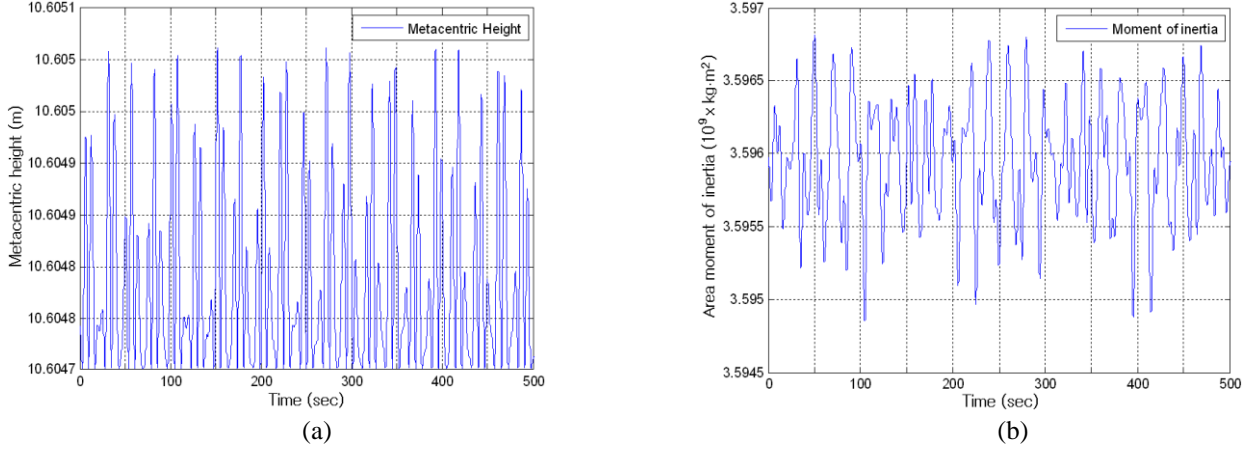
(a)   (b)

Fig. 5 The change to the platform motion ($\Omega = 0.1$ Hz): (a) metacentric height $\overline{GM_\theta}$, (b) area moment of inertia I_w of the wet part

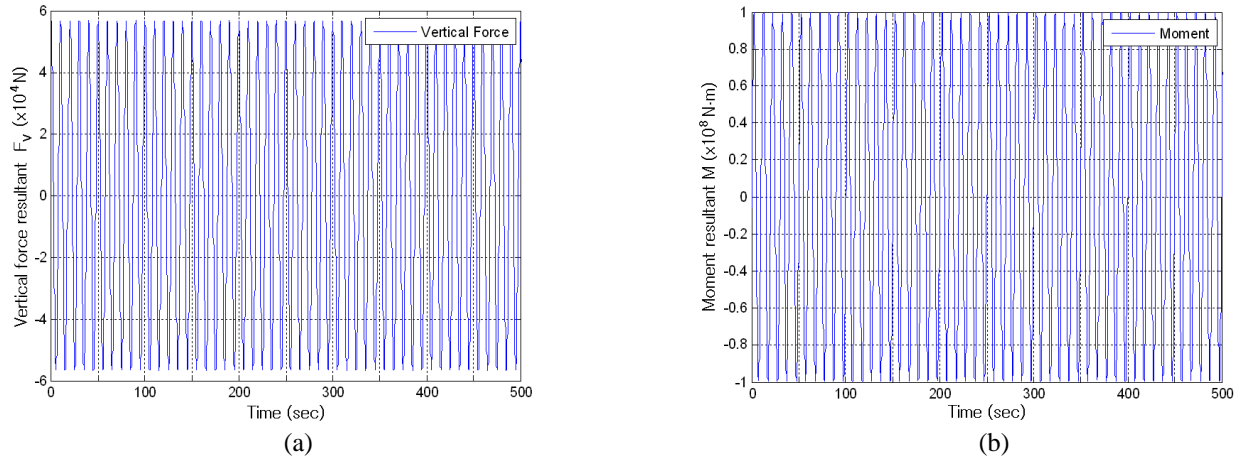(a)   (b)

Fig. 6 The change to the platform motion ($\Omega = 0.1$ Hz): (a) vertical force resultant F_V, (b) moment resultant M
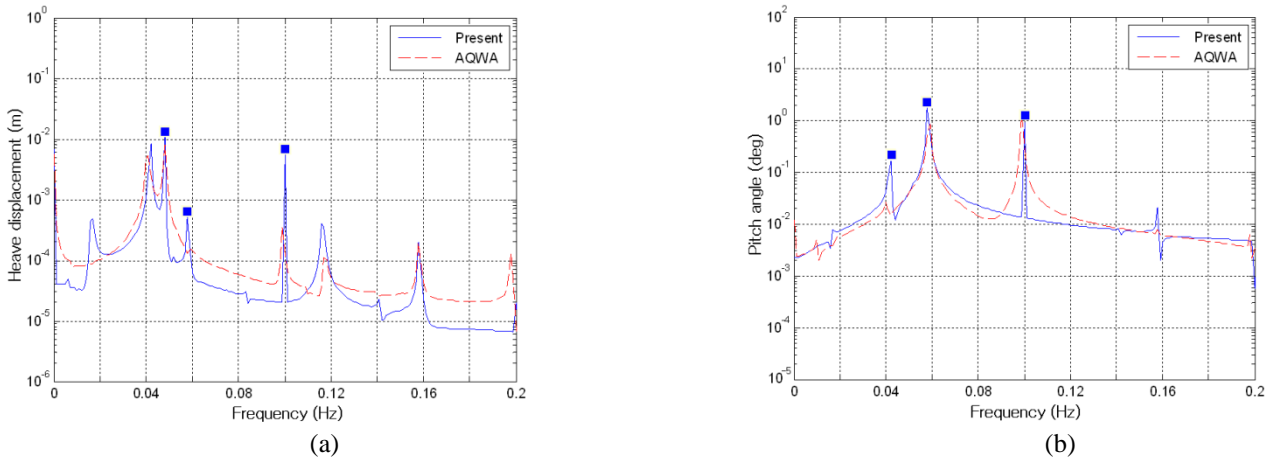

(a)   (b)

Fig. 7 Comparison of frequency responses to the wave frequency Ω of 0.1 Hz (solid lines: present method, dotted lines: AQWA): (a) heave response, (b) pitch response

time variation of hydrodynamic pressure, as represented in Eq. (21).

The transient time responses shown in Fig. 4 of the floating platform were transformed into the frequency domain by the digital Fourier transform (DFT), as represented in Fig. 7. Where, the frequency responses
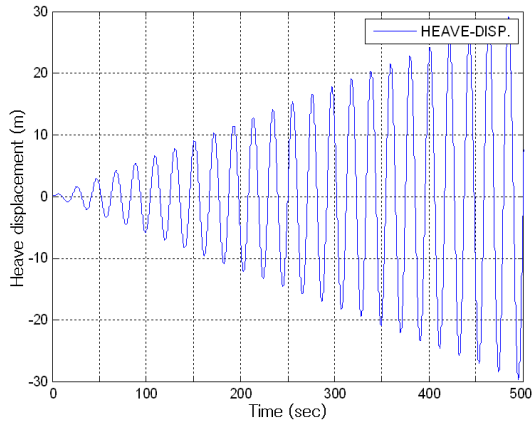
obtained by Ansys AQWA (2012) with damping are also included in order for the comparison with and without damping. First of all, it is observed that the present method and AQWA show a good agreement in the dominant peaks in both heave and pitch frequency responses. However, in case of AQWA, the insiginificant side peaks are not shown

and the magnitude of dominant peaks are relatively smaller owing to the inclusion of damping. So, in aspect of the parametric resonance, the numerical accuracy of the present method has been jusfied from the comparison with AQWA.
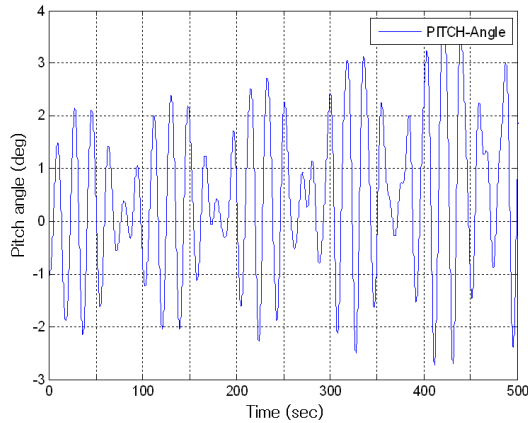
Meanwhile, It is clearly observed from Fig. 7 that each response shows two peaks at the wave frequency Ω and its own natural frequency (i.e., $\omega_h = 0.048$ Hz for heave motion, $\omega_p = 0.058$ Hz for pitch motion). Furthermore, each response shows the peak at the natural frequency of its counterpart motion, the peak at ω_p in the heave response and the peak at ω_h in the pitch response, respectively. Thus, it is clearly observed from the coupling between heave and pitch motions, which justifies that the coupling in resonance between two motions of floating platform is appropriately represented by the present nonlinear coupled equations.

4.2 Resonance in heave and pitch motions

Next, the resonance characteristics of floating platform are investigated with respect to the wave frequency. Figs. 8(a) and 8(b) represent the heave and pitch time responses when the wave frequency Ω is set by the heave natural frequency ω_h. The heave motion shows a clear typical resonance response, furthermore it is observed that 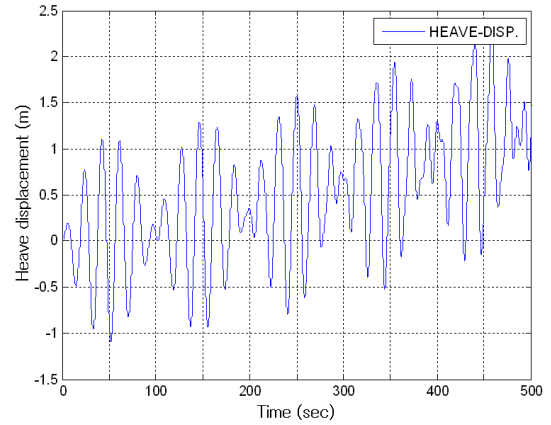the ampli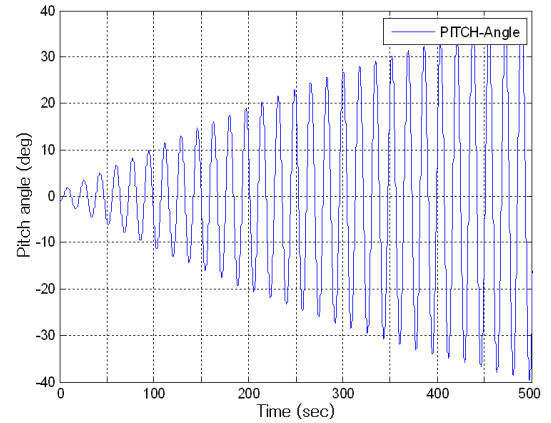tude of pitch motion in beating pattern uniformly increases with the lapse of time. Thus, it is found that the heave resonance produces an additive resonance with beating pattern in pitch motion.

This kind of coupling in resonance between heave and pitch motions is also observed from Fig. 9 when the wave frequency is set by the pitch natural frequency ω_p. The heave amplitude shows the gradual increase in beating pattern, and the floating platform gradually moves upwards. From the comparison between Figs. 8(b) and 9(a), it is observed that the coupled resonance at the heave natural frequency is weaker than one at the pitch natural frequency. Thus, it has been found that the influence on the coupling in resonance by pitch motion is stronger than that by heave motion.

In order to justify the coupling in resonance between heave and pitch motions, the heave and pitch time responses are parametrically investigated by changing the wave frequency from $0.045 Hz$ to $0.061 Hz$ with the frequency interval of $0.003 Hz$, and the time responses are transformed into the frequency domain. Figs. 10(a) and 10(b) represent the heave and pitch frequency responses for five different wave frequencies. The heave motion shows a peak at its natural frequency ω_h when excited by the heave natural frequency ($\Omega = \omega_h$), and it shows the peaks at the excitation frequency and the double excitation frequency as well as at its natural frequency when excited by the pitch

(a)

(b)

Fig. 8 Transient responses when the excitation frequency is the heave natural frequency ($\Omega = \omega_h$): (a) heave, (b) pitch

(a)

(b)

Fig. 9 Transient responses when the excitation frequency is the pitch natural frequency ($\Omega = \omega_p$): (a) heave, (b) pitch
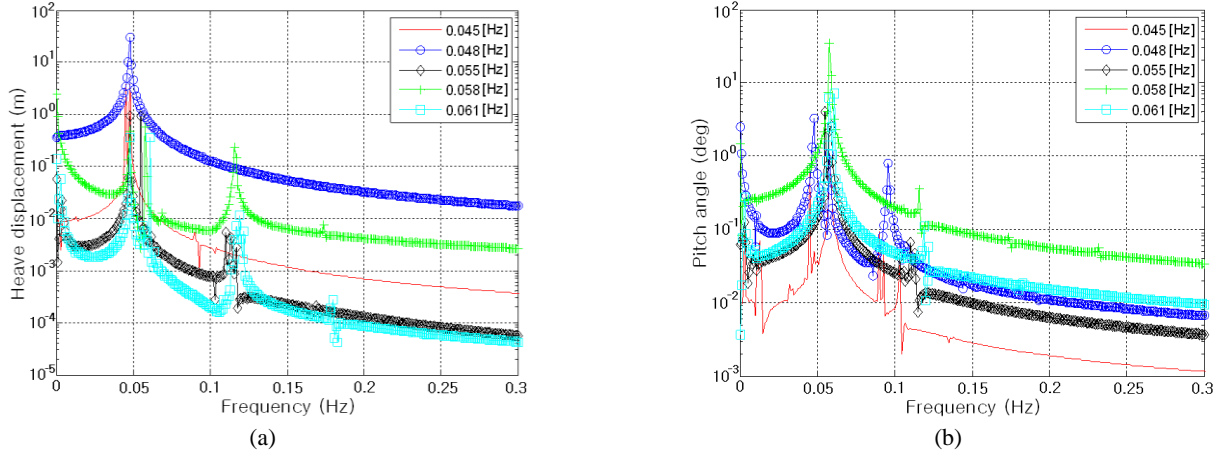
Fig. 10 The change of frequency response to the excitation frequency Ω : (a) heave, (b) pitch
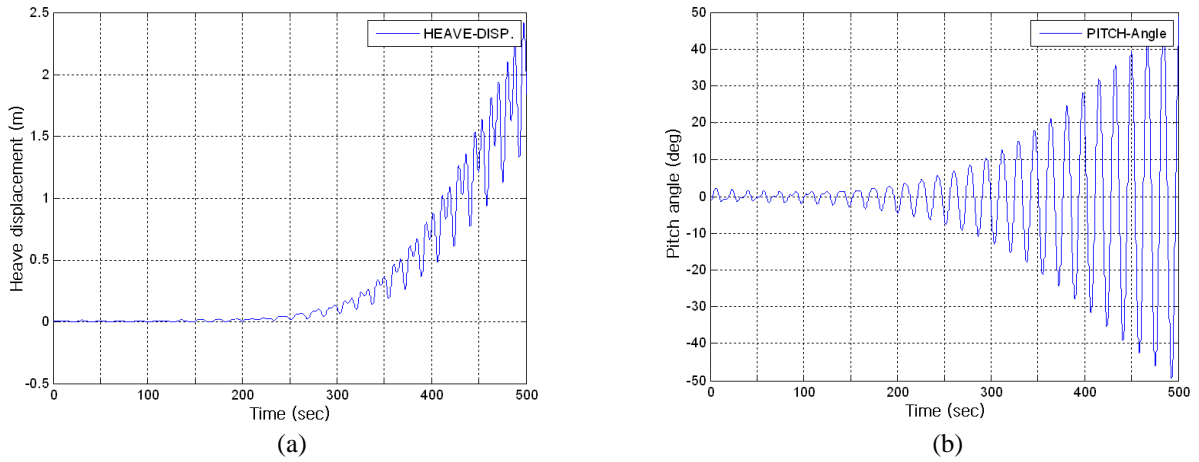

Fig. 11 Transient responses when excitation frequency is double pitch natural frequency ($\Omega = 2\omega_p$): (a) heave, (b) pitch
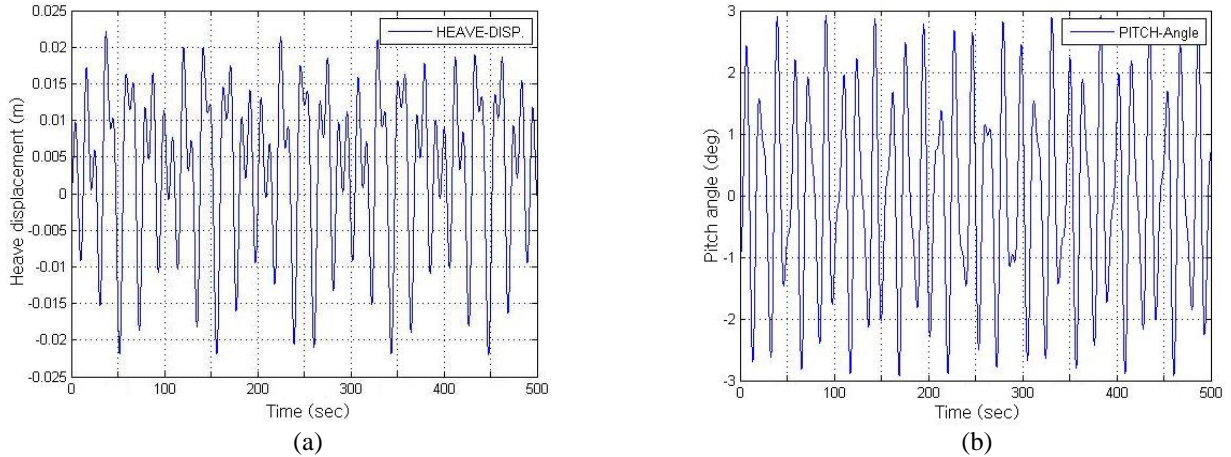

Fig. 12 Transient responses when excitation frequency is double heave natural frequency ($\Omega = 2\omega_h$): (a) heave, (b) pitch

natural frequency ($\Omega = \omega_p$). Meanwhile, the pitch motion produces the peaks at the double excitation frequency as well as at the excitation frequency when excited by the pitch natural frequency ($\Omega = \omega_p$), differing from the heave motion. However, it produces the peaks at the excitation and double excitation frequencies as well as at its natural frequency when excited by the heave natural frequency ($\Omega = \omega_h$). Thus, the coupling in the primary resonance (i.e.,

the resonance at the natural frequency of floating platform) between heave and pitch motions has been clearly justified. Next, the resonance characteristics of floating platform to the double natural frequencies of the floating platform are investigated. Figs. 11(a) and 11(b) represent the heave and pitch time responses respectively when the wave frequency becomes the double pitch natural frequency ($\Omega = 2\omega_p$). The pitch motion shows a clear resonance response, and

furthermore it produces the gradual upward movement with the increasing amplitude in heave motion. So, it is found that the wave excitation at the double pitch natural frequency does also give rise to the coupling in resonance between pitch and heave motions. Figs. 12(a) and 12(b) represent the transient time responses when the wave frequency is the double heave natural frequency ($\Omega = 2\omega_h$). One can observe that neither heave motion nor pitch motion produces the resonance phenomenon, differing from Fig. 11. Thus, it has been found that the wave excitation produces the resonance response in pitch motion and the coupled resonance response in heave motion only at the double pitch natural frequency.

5. Conclusions

In this study, the resonance characteristics of cylindrical floating platform in 2-D surface wave have been numerically investigated using a time-effective coupled nonlinear equations which is expressed by only two degrees of freedom. The floating platform was simplified as a undamped rigid body with two DOFs, and the coupled nonlinear dynamic equations were derived based on the small-amplitude wave potential and floating dynamic motion. The hydrodynamic interaction between the wave and the platform was modeled by the added mass, and the change in both the metacentric height and the area moment of inertia was considered. The transient time responses were calculated by the fourth-order Runge-Kutta (RK4) method, and their frequency responses were obtained by the digital Fourier transform.

Through the numerical experiments, it has been found that the heave and pitch motions produce not only the primary resonances by their natural frequencies but the coupled resonances by their counterpart natural frequencies. This coupling in resonance between heave and pitch motions does also occur when the wave frequency becomes the double pitch natural frequency. But, the wave frequency equal to the double heave natural frequency produces neither the resonance in heave motion nor the coupled resonance in pitch motion. And, it has been found that the pitch motion gives rise to more significant effect on the coupled resonance than the heave motion.

Acknowledgements

References

Ansys AQWA. (2012), Available from: (http://www.ansys.com/products/aqwa/).

Browning, J.R., Jonkman, J., Robertson, A. and Goupee, A.J. (2014), "Calibration and validation of a spar-type floating offshore wind turbine model using the FAST dynamic simulation tool", *J. Physics, Conference Series*, **555**(1), 012015.

Cho, J.R., Song, J.M. and Lee, J.K. (2001), "Finite element techniques for the free-vibration and seismic analysis of liquid-storage tanks", *Finite Elem. Anal. Des.*, **37**(6), 467-483.

Choi, E.Y., Cho, J.R., Cho, Y.U., Jeong, W.B., Lee, S.B., Hong, S.P. and Chun, H.H. (2015), "Numerical and experimental study on dynamic response of moored spar-type scale platform for floating offshore wind turbine", *Struct. Eng. Mech.*, **54**(5), 909-922.

Chujo, T., Ishida, S., Minami, Y., Nimura, T. and Inoue, S. (2011), "Model experiments on the motion of a SPAR type floating wind turbine in wind and waves", *ASME 2011 International Conference Ocean Offshore Arctic Eng. OMAE2011*, 655-662.

Currie, I.G. (1974), *Fundamental Mechanics of Fluids*, New York, McGraw-Hill.

Dean, R.G. and Dalrymple, R.A. (1984), *Water Wave Mechanics for Engineers and Scientists*, New Jersey, Prentice-Hall.

Faltinsen, O.M. (1990), *Sea Load on Ships and Offshore Structures*, University of Cambridge.

Haslum, H.A. and Faltinsen, O.M. (1999), "Alternative shape of spar platforms for use in hostile areas", *Offshore Technology Conference OTC-10953-MS*.

Hong, Y.P., Lee, D.Y., Choi, Y.H., Hong, S.K. and Kim, S.E. (2005), "An experimental study on the extreme motion responses of a spar platform in the heave resonant waves", *Fifteenth International Ocean Polar Engineering Conference ISOPE-I-05-033*.

Irani, M.M. and Finn, L. (2004), "Model testing for vortex induced motions of spar platforms", *ASME 2004 International Conference Offshore Mech. Artic Eng. OMAE2004-51315*, 605-610.

Jeon, S.H., Cho, Y.U., Seo, M.W., Cho, J.R. and Jeong, W.B. (2013), "Dynamic response of floating substructure of spar-type offshore wind turbine with catenary mooring cables", *Ocean Eng.*, **72**, 356-364.

Karimirad, M., Meissonnier, Q. and Gao, Z. (2011), "Hydroelastic code-to-code comparison for a tension leg spar-type floating wind turbine", *Marine Struct.*, **24**(4), 412-435.

Koo, B.J., Kim, M.H. and Randall, R.E. (2004), "Mathieu instability of a spar platform with mooring and risers", *Ocean Eng.*, **31**(17-18), 2175-2208.

Kyoung, J.H., Hong, S.Y., Kim, B.W. and Cho, S.K. (2005), "Hydroelastic response of a very large floating structure over a variable bottom topology", *Ocean Eng.*, **32**(17), 2040-2052.

Liao, S.W. and Yeung, R.W. (2001), "Investigation of the Matheiu instability of roll motion by a time-domain viscous-fluid method", *16th International Workshop Water Waves Floating Bodies*, 97-100.

Matos, V.L.F., Simos, A.N. and Sphaier, S.H. (2011), "Second-order resonant heave, roll and pitch motions of a deep draft semi-submersible: Theoretical and experimental results", *Ocean Eng.*, **38**(17-18), 2227-2243.

Radhakrishnan, S., Datla, R. and Hires, R.I. (2007), "Theoretical and experimental analysis of tethered buoy instability in gravity waves", *Ocean Eng.*, **34**(2), 261-274.

Rho, J.B., Choi, H.S., Lee, W.C., Shin, H.S. and Park, I.K. (2002a), "Heave and pitch motions of a spar platform with damped plate", *Twelfth International Ocean Polar Engineering Conference ISOPE-1-02-031*.

Rho, J.B., Choi, H.S., Shin, H.S. and Park, I.K. (2002b), "A study on Mathieu-type instability of conventional spar platform in regular waves", *Twelfth International Ocean Polar Engineering Conference ISOPE-05-15-2-104*.

Roddier, D., Cermelli, C., Aubault, A. and Weinstein, A. (2010), "WindFloat: A floating foundation for offshore wind turbines", *J. Renew. Sustainable Energy*, **2**(3), 033104.

Sorensen, R.M. (1978), *Basic Coastal Engineering*, New York, John Wiley.

Tong, K.C. (1998), "Technical and economic aspects of a floating

offshore wind farm", *J. Wind Eng. Indust. Aerodyn.*, **74-76**, 399-410.

Ye, X., Gao, Z., Moan, T. and Zhang, L. (2014), "Comparison of numerical and experimental analyses of motion response of a spar-type floating offshore wind turbine in waves", *Twenty-fourth International Ocean Polar Engineering Conference* ISOPE-I-14-085.

CC